ARCHIVES OF ACOUSTICS
21, 2, 195–200 (1996)

MICROPROBE TECHNIQUES IN SAW MEASUREMENTS

E. CHILLA, T. HESJEDAL and H.-J. FRÖHLICH

Paul-Drude-Institut für Festkörperelektronik
(D-10117 Berlin, Germany)

Starting from the conventional microprobe techniques, a scanning acoustic tunneling microscope (SATM) and a scanning acoustic force microscope (SAFM) have been developed to detect particle displacements at solid surfaces up to GHz frequencies. Based on the non-linear dependence of the tunneling current in SATM and of the forces in SAFM on the tip to surface distance, respectively, it is demonstrated that wave field parameters of surface acoustic waves can be measured with a lateral resolution in the submicrometer range.

1. Introduction

Many different methods to measure amplitude and phase of surface acoustic waves (SAWs) are available. One of the well established non-contact methods is the laser optical probing. The spatial resolution of this method is given by the minimum achievable spot diameter which is practically of the order of some micrometers [1]. A better resolution, needed for the inspection of high frequency SAWs, can be realised by using the scanning acoustic tunneling microscope (SATM) [2] as well as the scanning acoustic force microscope (SAFM) [3] as a local probe.

Bulk acoustic wave pulses up to several MHz were analysed by an electron tunneling probe [4]. The acoustic amplitude was detected by the contrast variation of a scanning tunneling microscope (STM) image due to acoustic vibration [5]. Amplitude modulated SAWs near 90 MHz were received by a combined boxcar and lock-in technique [6]. First ideas of the phase accurate probing of SAWs using a modified STM were given in 1989 [7]. This SATM utilises an additional rf signal at the tunneling tip leading to a frequency mixing. Amplitude and phase of the ac tunneling current component at the difference frequency were measured at a fixed probe position by an oscilloscope [8]. Strong local variations of the phase were resolved by replacing the oscilloscope by a lock-in amplifier [9, 10]. Measuring at the difference frequency overcomes the limited bandwidth of the STM and reduces the influence of the inevitable displacement current [8, 11]. Nonlinear contributions to the dc and ac components of the tunneling current must be taken into account for SAWs with finite amplitude [11].

Because the SATM is limited to electrically conducting surfaces the SAFM has been developed to measure the amplitude of SAWs on arbitrary surfaces. First results were reported in 1991 [12]. In the so-called contact mode the lever can not follow the surface oscillation at frequencies being sufficiently higher than the lever mechanical resonance frequency. Nevertheless, an output signal is delivered in this case by a shift of the mean lever position [13–15]. The deviation of this position from the position without SAW depends non-linearly on the SAW amplitude.

In this contribution experimental setups for the SATM and the SAFM are described and examples of their application in SAW measurements are demonstrated and discussed.

2. Scanning acoustic tunneling microscope

Figure 1 shows a schematic diagram of the experimental setup. The output voltages of the two rf generators tuned to the SAW frequency f_a and to the modulation frequency f_v of the gap voltage are fed via variable attenuators to the interdigital transducer (IDT) and the tunneling tip, respectively. Additionally, these voltages are fed to a mixing stage. The output signal of this stage which contains the difference frequency supplies the reference channel of a lock-in amplifier. The ac component of the tunneling signal which is generated by the propagating SAW below the tip is fed to the signal input of the lock-in which delivers the amplitude as well as the phase of the SATM signal at the difference frequency. The sample to be

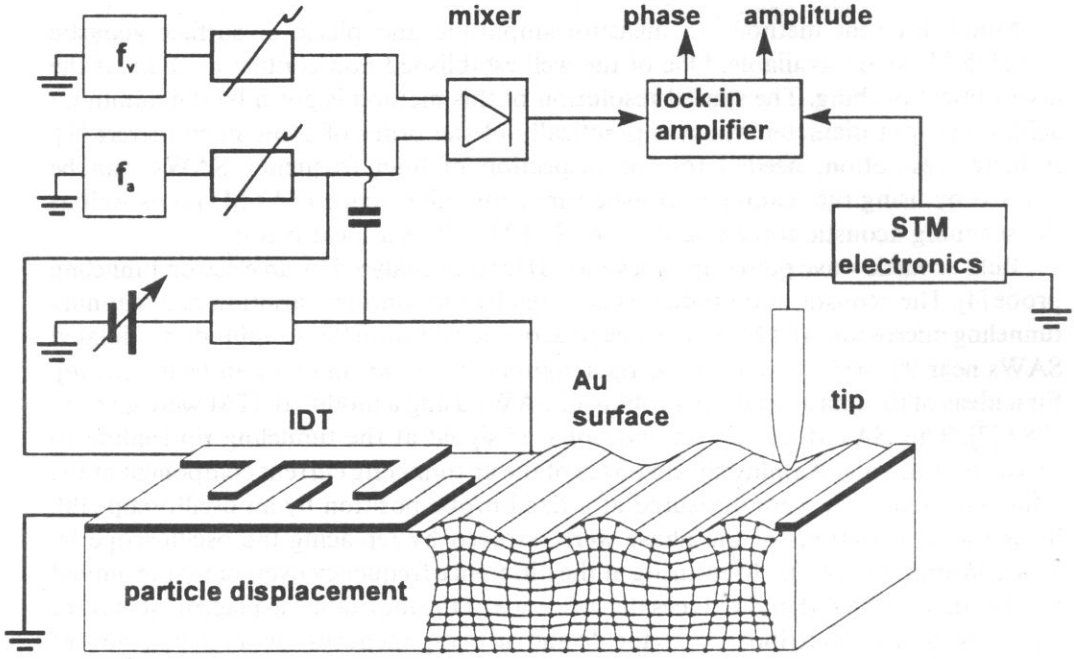

Fig. 1. SATM with gap voltage modulation.

investigated must have an electrically conducting surface to ensure the tunneling current. To avoid disturbing thin oxide coatings the metallization of the SAW propagation path is made by evaporating a thin gold layer.

As an example of a SATM application Fig. 2 displays the phase output signal of the lock-in in dependence on the SAW frequency. The tip of the SATM was positioned at the metallized part of a SAW delay line on $LiNbO_3$. The SAW of

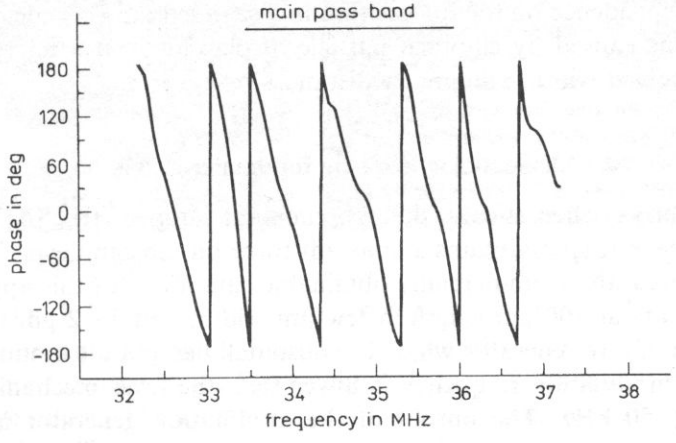

Fig. 2. Phase of a SAW delay line measured by SATM.

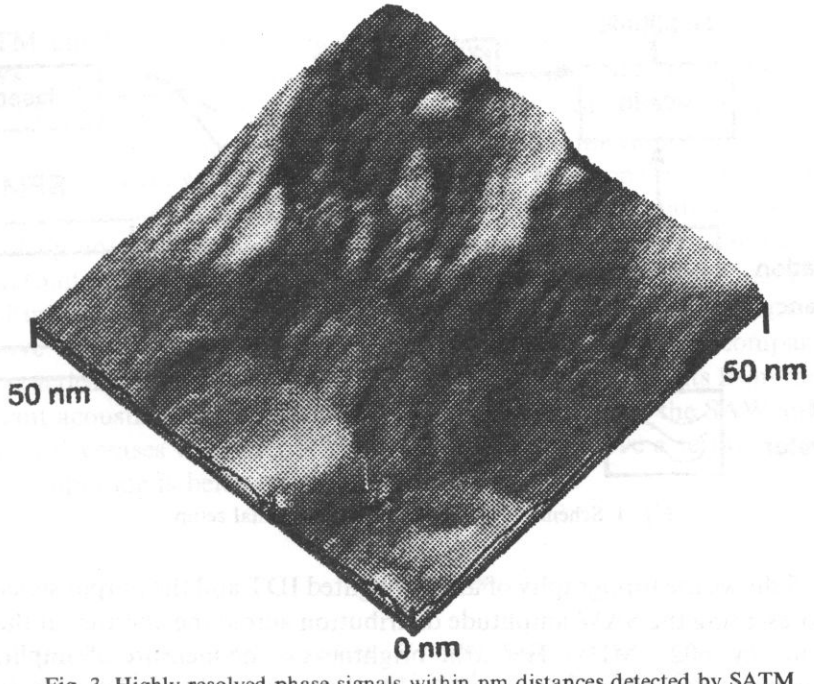

Fig. 3. Highly resolved phase signals within nm distances detected by SATM.

Rayleigh-type was excited by an IDT. The found phase behaviour is typical for delay lines and corresponds also with the estimation of the phase shift as a function of the frequency at known phase velocity and distance between the tip position and the middle of the IDT. It should be noted that the phase is also well imaged outside of the main pass band of IDT which is marked by the arrow. Another SATM application is shown in Fig. 3. There the phase signal of the lock-in is imaged at constant SAW frequency in dependence on the tip position in a scanned area of a delay line. Strong phase variations caused by elliptical particle displacement at a microcsopic rough surface are resolved within nanometer distances.

3. Scanning acoustic force microscope

Figure 4 shows schematically the experimental setup of the SAFM in contact mode. A feedback loop maintains a constant force on the cantilever. Typical forces are some hundred nN. Commercially obtainable cantilever for this application have dimensions of about 100 μm length, a few μm width, and 1–2 μm thickness. The output voltage of a rf generator which is sinusoidally amplitude modulated is fed to the IDT. The modulation frequency is lower than the lever mechanical resonance frequency, e.g. 50 kHz. The output of the modulation generator is additionally connected with the reference input of the lock-in. The output signal of a segmented photo diode which optically measures the deflection of the cantilever is fed to the signal input channel of the lock-in.

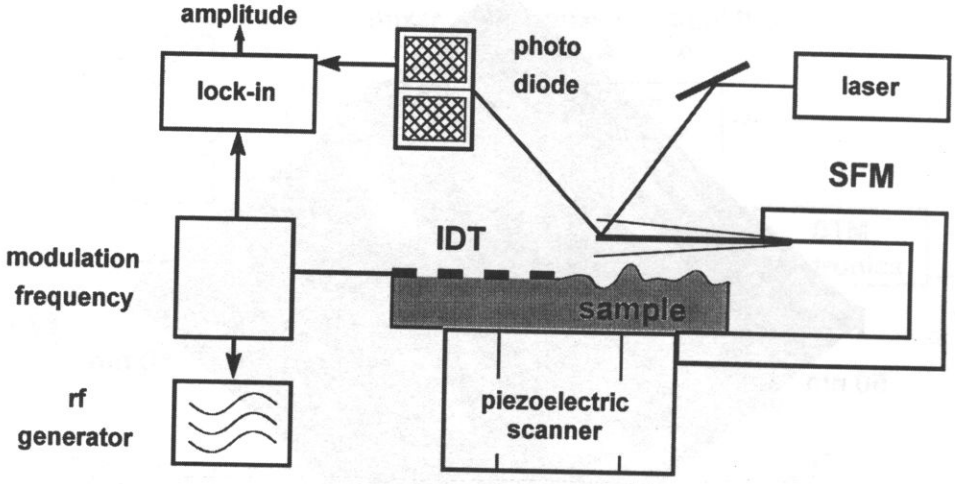

Fig. 4. Schematic of the SAFM experimental setup.

Figure 5 shows the topography of an unweighted IDT and the output signal of the lock-in representing the SAW amplitude distribution across the aperture at the IDT's centre frequency (602.7 MHz). Here, the brightness is the measure of amplitude. In vertical direction the periodic appearance of brightness maxima reflects the standing

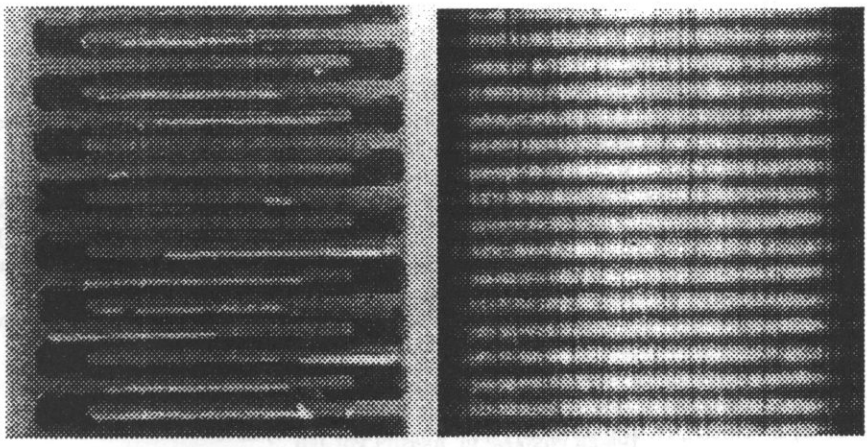

Fig. 5. Amplitude distribution within an IDT measured by SAFM.

wave field within an IDT. Since the lock-in signal depends non-linearly but with a really unknown function on the SAW amplitude the instrument has to be calibrated for quantitative studies. The aperture of the IDT was 26 μm, the scans were formed by 256 points per line. The substrate material was STX quartz.

4. Discussion

SATM and SAFM were demonstrated to be suitable instruments for the detection of SAWs. Applied frequencies were at 35 MHz (SATM) and at 600 MHz (SAFM). An upper frequency limit for the SATM might set in sooner by technical problems of supplying the tunneling gap with a rf signal for the mixing than by the time constant of the tunneling effect which is in the order of 10 fs. Frequencies up to the microwave K band should be applicable. The minimum detectable amplitude with the described setup not optimised in relation to the signal to noise ratio was near 10^{-4} nm. The spatial resolution of amplitude and phase signals is better than 1 nm and is described in detail in [16]. An upper frequency limit for the SAFM does not exist within the microwave range. Nevertheless, the lower amplitude sensitivity compared to the SATM practically limits also the detectable frequency. This results from the fact that at constant acoustic power density in typical SAW structures the SAW amplitude at the surface decreases with $(\text{frequency})^{-1/2}$ and, hence, above a certain frequency the resulting amplitude is below the detectable level.

References

[1] A. Ginter, G. Sölkner, Appl. Phys. Lett., **56** (1990), 2295.
[2] T. Hesjedal, E. Chilla, H.-J. Fröhlich, Thin Solid Films, **264** (1995), 226.

[3] E. CHILLA, T. HESJEDAL, H.-J. FRÖHLICH, in Proc. IEEE Ultrasonics Symposium 1994, 363.
[4] A. MOREAU, J.B. KETTERSON, J. Appl. Phys., **72**, (1992), 861.
[5] J. HEIL, J. WESNER, W. GRILL, J. Appl. Phys., **64** (1988) 1939.
[6] S.E. MCBRIDE, C.G. WETSEL, Jr., in Proc. IEEE Ultrasonics Symposium 1992, 445.
[7] E. CHILLA, H.-J. FRÖHLICH, J. RIEDEL, W. ROHRBECK, in Proc. 8. Tagung Akustik/11. Winterschule Mikroakustik (Phys. Gesellschaft d. DDR), 1989, 212 (in German).
[8] W. ROHRBECK, E. CHILLA, J. RIEDEL, H.-J. FRÖHLICH, Appl. Phys., **A 52** (1991) 344.
[9] E. CHILLA, W. ROHRBECK, H.-J. FRÖHLICH, R. KOCH, K.H. RIEDER, Appl. Phys. Lett. **61** (1992) 3107.
[10] E. CHILLA, W. ROHRBECK, H.-J. FRÖHLICH, R. KOCH, K.H. RIEDER, Annalen der Physik, **3** (1994), 21.
[11] H.-J. FRÖHLICH, E. CHILLA, in Proc. European Workshop on High Frequency Ultrasonic Information Processing, Valenciennes/France, February 17–18, 1994.
[12] W. ROHRBECK, E. CHILLA, H.-J. FRÖHLICH, J. RIEDEL, Abstr. of International Conference on Scanning Tunneling Microscopy, Interlaken/Switzerland, August 12–16, 1991, 52.
[13] W. ROHRBECK, E. CHILLA, Phys. Status Solidi (a), **131** (1992) 69.
[14] O. KOLOSOV, K. YAMANAKA, Jpn. J. Appl. Phys. **32** (1993) L1095.
[15] T. HESJEDAL, E. CHILLA, H.-J. FRÖHLICH, Appl. Phys., **A 61** (1995) 237.
[16] T. HESJEDAL, E. CHILLA, H.-J. FRÖHLICH, submitted to Appl. Phys. Lett.